

# **An Investigation into Different Correlation Methods between NMR T<sub>2</sub> Distributions and Primary Drainage Capillary Pressure Curves Using an Extensive Sandstone Database**

Adam K Moss – AKM Geoconsulting, Tim Benson – Advanced Magnetic Resonance,  
Tony Barrow – Weatherford Laboratories

*This paper was prepared for presentation at the International Symposium of the Society of Core Analysts held in Trondheim, Norway, 27-30 August 2018*

## **ABSTRACT**

Many workers have recognised the link between Nuclear Magnetic Resonance (NMR) derived T<sub>2</sub> distributions and pore size distributions in reservoir rocks. This property has been used to develop models to obtain primary drainage capillary pressure curves from T<sub>2</sub> distributions. These models often assume that the rocks pore space resembles a simple bundle of capillary tubes. They do not consider the existence of multiple pore body connections and pore body restrictions/throats. The most successful models utilise variable scaling factors to convert T<sub>2</sub> times to pore diameters and hence capillary pressure. The variable scaling factor approach recognises the existence of variable surface relaxivity throughout the pore space due to variations in mineralogy and pore topography.

This investigation uses SCAL data from the ART NMR Sandstone Rock Catalogue to obtain core calibrated variable scaling factors for 174 reservoir sandstone samples. The depositional environments for these samples include; aeolian, fluvial, coastal and shallow and deep marine. The samples used have a wide variety of mineralogy, diagenetic overprints and cover six orders of magnitude in absolute permeability. Three different methods for obtaining the scaling factors are presented and the relative merits of each discussed. A global model to predict capillary pressure from NMR T<sub>2</sub> distributions in reservoir sandstones has been developed using correlations between the variable scaling factors and permeability.

## **INTRODUCTION**

Nuclear Magnetic Resonance (NMR) measurements have been used extensively to characterise reservoir rock pore geometry using logging and lab-based NMR spectrometers [1]. The sensitivity of the NMR measurement to pore-size distribution potentially enables capillary pressure to be modelled from NMR data. Several workers have proposed methods to derive drainage capillary pressure vs saturation curves from NMR data [2-4]. This paper expands this theory and model types.

NMR measures the relaxation behaviour of hydrogen nuclei [5]. In this study, we utilise the T<sub>2</sub> relaxation of the hydrogen nuclei. In most porous rock systems, there will be a continuous range of pore sizes, rather than several discrete sizes. In fully brine saturated

rocks each pore-size has a distinctive  $T_2$  value. The NMR response to one pore-size will have a characteristic  $T_2$  value and signal amplitude proportional to the amount of fluid contained in pores of that size.

In a water-wet rock, relaxation of hydrogen nuclei in the water occupying the smallest pores occurs, because of interaction with the pore surfaces. Part of the  $T_2$  distribution relates to water in pores which could be displaced by hydrocarbons and part relates to capillary-bound water. The  $T_2$  cut-off method is often used to define capillary bound water volumes. Using a  $T_2$  cut-off value to define capillary bound water for NMR logs will assume that all rocks are at an irreducible water saturation. Therefore, to use NMR logs to accurately define water saturations it is beneficial to convert the NMR  $T_2$  distributions to capillary pressure curves at each depth. Knowing the height above free water level allows us to use the capillary pressure curves to estimate water saturation at each depth without the need to revert to a  $T_2$  cutoff or irreducible water saturations concepts.

## MERCURY INJECTION VS NMR

Mercury injection utilises the very high interfacial tension between mercury and air to produce extremely high capillary pressure and obtain low wetting phase saturations. Most commercially available mercury injection porosimeters can apply a mercury injection capillary pressure up to 60,000psia. This is a high enough capillary pressure to fill a pore of 0.0036 microns diameter with mercury. Details on mercury injection theory and experimentation can be found in Shafer & Neasham (2000) [6]. Mercury injection capillary pressure (MICP) curves can be converted to a pore size distribution by rearranging the Washburn equation, Equation 1.

$$r = \frac{-C \ 2\sigma \cos\theta}{P_{cMICP}} \quad (1)$$

Where:  $r$  = Pore radius (microns),  $P_{cMICP}$  = Mercury injection capillary pressure (psia),  $\sigma$  = Mercury/air interfacial tension (dynes/cm),  $\theta$  = Contact angle between the mercury/air interface & the rock (degrees),  $C$  = A unit conversion factor

Marschall et al (1995) [2] noted that the pore size distribution obtained from mercury injection data could be ‘scaled’ to NMR  $T_2$  distribution data for the same sample using a ‘scaling factor’ of unit microns/ms, Equation 2. They called the scaling factor an effective relaxivity ( $Rho$ ) and stated that it was proportional to the samples intrinsic surface relaxivity and the pore-throat size body ratio.

$$\text{Scaling Factor, } Rho \text{ (microns/ms)} = \frac{-C \ 2\sigma \cos\theta}{P_{cMICP} \times T_2} \quad (2)$$

Using a single scaling factor assumes that a linear relationship exists between pore throat radius and pore body size. Figure 1 shows a sandstone example in which a single scaling factor of 0.04 microns/ms works reasonably well at modelling the capillary pressure

curve even though mercury injection pore size distribution and saturated sample  $T_2$  distributions have different shapes. The scaling factor in the example in Figure 1 was obtained by manually moving one distribution over the other until it looks like there is a ‘good’ fit. This manual fitting is very subjective, and the results will differ between operators. A less subjective single scaling factor can be obtained by calculating the ratio of the median pore size (diameter at 50% mercury saturation) from the mercury injection curve and the log mean  $T_2$  value from the brine saturated  $T_2$  distribution, Equation 3. We refer to this type of scaling factor as  $Rho_{simple}$

$$Rho_{simple} \text{ (microns/mS)} = \frac{\text{Median Pore Diam (microns)}}{\text{Mean } T_2 \text{ (mS)}} \quad (3)$$

One criticism of using the methods described above to calculate the scaling factors is that the pore size distributions from the mercury injection data and the NMR  $T_2$  distribution from the CPMG echo train data are derived in very different ways. The mercury injection pore size is usually obtained by calculating the volume intrusion at each incremental pressure step. The shape of the resulting distribution is dependent on the number and ‘spacing’ of the pressure steps. The resulting pore size distribution is often ‘spikey’ as can be seen in Figure 1. A full discussion on different methods for deriving pore size distributions from mercury injection data can be found in Lenormand 2003 [7]. The  $T_2$  distribution is derived from an inversion of the multi exponential decay CPMG echo-train.

Hence it is not appropriate to compare the standard forms of both the distributions.

We propose a new simplified method based on matching NMR time domain data and reconstructed MICP time domain data which removes some of the issues associated with other matching techniques. To the authors knowledge this is the first published use of MICP time domain data. To match in the time domain, first the MICP pore size distribution data must be transformed into a sum of exponential functions with time constants based on pore sizes. This is done via the Equation 4.

$$R(t_i) = \sum_{j=1}^m G_j \cdot e^{\frac{-t_i}{Y \cdot A_j}} \quad (4)$$

Where  $G_j$  is the MICP distribution amplitude at the particular pore size  $A_j$ . Equation 4 is evaluated for  $t_i$  values corresponding to the NMR echo acquisition times. This process, unlike the reverse process of inversion, is simple to perform and has the advantage of allowing the number of points to be chosen to precisely match the acquired NMR time domain data.  $Y$ , a parameter related to the surface relaxivity, can then be obtained by choosing a value for  $Y$  such that:

$$M(t_i) - R(t_i) = 0 \quad (5)$$

Where  $M(t_i)$  are the echo amplitudes of the corresponding NMR data at time  $t_i$ .  $Y$  can either be single valued, or a more complex function could be substituted. The single value surface relaxivities obtained using this method will be referred to as the  $\text{Rho}_{\text{Inversion Model}}$ .

Figures 2a & 2b shows the result of two matches between NMR and MICP time domain data. Figure 2a shows a good fit and negligible difference between the NMR and MICP data. Figure 2b shows a poor fit, indicating either that the single value model for  $Y$  is inappropriate, or indicative of the fact that NMR and MICP are not measuring identical pore systems. Once the time domain match is established, both data sets can then be inverted to recover the pore size distributions. Although this process effectively removes resolution in the inverted MICP data set compared to the original data, it has the benefit that identical smoothing via the regularisation parameter is applied to both the NMR and the MICP data which allows a better assessment of the quality of the match.

Figure 3a shows the NMR  $T_2$  distribution data and original MICP distribution data of the core from Figure 2a and Figure 3b the data after time domain matching and inversion for the same core. The first core displays very little difference between the NMR and MICP pore size distributions after inversion as expected, whereas the core from Figure 2b displayed in Figures 4a and 4b shows significant differences, which may be explained either by pore coupling or pore shielding.

The single scaling factor methods can not be used in samples which contain a range of surface relaxivities due to complex mineralogy and a distribution of pore-throat size body ratios. To account for these effects the variable scaling factor method was developed by Volokitin et al (1999) [4]. The method uses a scaling factor for every saturation point. Thus ‘forcing’ the  $T_2$  distribution to match the capillary pressure curve, Figure 5. The scaling factor for each saturation point is the multiplier needed to convert the  $T_2$  time to the equivalent capillary pressure. This method has been recently used by Brandimarte et al (2017) [8] to successfully model water saturation using the NMR log in a heterogeneous carbonate light oil and condensate reservoir. The method assumes that the NMR log  $T_2$  distribution reflects the rocks pore size distribution and is not dominated by non-wetting phase fluid responses. This is more probable in gas or water-wet light oil reservoirs drilled with water-based mud. An example of a scaling factor ( $\text{Rho}$ ) versus saturation function for the same sample as used in Figure 1 is presented in Figure 6. For convenience the data is re-plotted as scaling factor against  $T_2$  time. On a log-log plot a power equation gives a very good regression result, Figure 7. We refer to the model constructed using these relationships as the Variable  $\text{Rho}$  Model.

In this study we compare the results of using the three different methods of obtaining both single and variable scaling factors described above in a wide range of sandstone sample. We attempt to construct ‘global’ models which would allow NMR log  $T_2$  distribution data to be converted to capillary pressure versus saturation curves.

## THE DATA SET

Data from the ART NMR Sandstone Rock Catalogue is used in this study. The dataset includes 174 plug samples with high pressure mercury injection capillary pressure (MICP) curves and NMR  $T_2$  measurements on brine saturated plugs. The sandstone samples come from oil and gas reservoirs around the world. The depositional environments for these samples include; aeolian, fluvial, coastal and shallow and deep marine. The samples used have a wide variety of mineralogy and diagenetic overprints. Figure 8 shows the nitrogen permeability against helium porosity at zero confining pressure plot for the 174 samples. Permeability covers six orders of magnitude and porosity ranges from 0.03 to 0.33.

It should be noted that the brine saturated sample NMR  $T_2$  distributions were conducted on plug samples whilst the mercury injection tests were run on trims from these plugs. A comparison of these two data types to obtain scaling factors relies on the two samples having identical properties. In heterogeneous rocks and rocks with pores below the resolution (0.0036 microns) that the MICP can detect this may not be the case. Therefore, only samples in which the difference between the MICP porosity and the NMR porosity is less than 0.015 (1.5 porosity units) are used to construct the scaling factor models. Seventy-eight plugs sample meet this criterion, Figure 9. The nitrogen permeability against helium porosity plot, Figure 10, shows that a wide range of porosity and permeability is still maintained within this sub-set of seventy-eight plugs. X-ray diffraction mineralogy data was available for 23 of these samples.

## APPLICATION OF THE SCALING FACTOR MODELS

**Single Scaling Factor Models:** In this paper we evaluate two single scaling factor models,  $Rho_{simple}$  and  $Rho_{Inversion Model}$ . Equation 3 has been used to calculate the  $Rho_{simple}$  scaling factor for the seventy-eight plugs that had a porosity difference of less than 0.015 between NMR and MICP porosity. To construct a predictive ‘global’ model that can be applied to NMR log data we need to find a relationship between the  $Rho_{simple}$  values and common petrophysical properties i.e. porosity, permeability or clay content. For this sample set the only satisfactory relationship was between  $Rho_{simple}$  and nitrogen permeability, Figure 11.

The second single scaling factor method uses the reconstructed MICP data as produced by Equation 4. This is fitted to the raw (un inverted) NMR data to obtain a single value of  $\rho$  ( $Rho_{Inversion Model}$ ). The surface relaxivities obtained using the MICP inversion method were correlated against porosity, permeability and clay content. A weak relationship between  $Rho_{Inversion Model}$  and nitrogen permeability could be enhanced by dividing the data using flow zone index groups. Flow zone index (FZI) is defined by Equation 6, Amaefule et al. 1993 [9].

$$FZI = \frac{RQI}{\phi_z} \quad (6)$$

Where:  $RQI = 0.0314 * (K/\Phi)^{0.5}$ ,  $\Phi_z = \Phi / (1-\Phi)$ ,  $K$ =Nitrogen Permeability (mD),  $\Phi$ =Porosity (fraction)

The distribution of  $Rho_{\text{Inversion Model}}$  values is divided into those with a flow zone index value either greater or low than 0.83. These two groups are then plotted against nitrogen permeability and relationships obtained, Figure 12.

**Variable Scaling Factor Model:** The basis for the variable scaling factor model is a power equation fit to a plot of Rho against  $T_2$  time, Figure 7. The regression fit parameter ( $R^2$ ) is very good in this example, having a value of 0.98. The  $R^2$  values for these plots should be viewed with caution. They are potentially high because the Y parameter (psi/ms) is derived from the X parameter (ms). It is possible to obtain a ‘false’ correlation with this type of plot. Therefore, in this study we have only used the power equations that have an  $R^2$  value of 0.98 or higher. This means we can be sure we have data with ‘real’ not ‘false’ correlations. Using the individual plug power equations to predict the scaling factors at each  $T_2$  time we can construct modelled capillary pressure curves for each sample. Figure 13 compares measured and modelled mercury injection capillary pressure curves for selected samples. The quality of the fit between the measured and modelled mercury injection capillary pressure curves indicates that the correlations obtained from the Rho against  $T_2$  plots are not false/spurious correlations.

To construct a model that can be applied to NMR log data we need to correlate the multiplier and the power values in each plugs power equation with common petrophysical parameters. The power values were found to correlate reasonably well with nitrogen permeability if divided into samples with a flow zone index either greater or lower than 0.83, Figure 14. The multipliers in the power equations did not correlate with any petrophysical parameter so average values were obtained for the two flow zone index groups of samples. The following equations can be used to predict the scaling factor (Rho) for each  $T_2$  time.

For samples with a flow zone index less than 0.83:

$$Rho = 16,080 T_2^{-2.189} K^{0.035} \quad (7)$$

For samples with a flow zone index greater than 0.83:

$$Rho = 20,457 T_2^{-2.0256} K^{0.0247} \quad (8)$$

*Rho=Surface Relaxivity (psi/ms),  $T_2$ = $T_2$ relaxation time (ms),  $K$ =Nitrogen Permeability (mD)*

The three models for predicting the scaling factors, Rho Simple Model, MICP Inversion Rho Model and the Variable Rho Model, have been applied to the saturated sample NMR  $T_2$  data for a set of six samples. The samples cover a nitrogen permeability range of 1720 to 0.05mD and an NMR porosity range from 0.33 to 0.08. The modelled capillary pressure curves are compared with measured in Figure 15. Given the low  $R^2$  correlation values for the global model equations in Figures 11, 12 and 14 the quality of fits in Figure 15 is promising. The overall quality of fit of each modelled capillary pressure curve is determined by calculating the mean saturation difference between modelled and measured curves, Table 1. Using overall quality of fit for this set of samples the variable

Rho model is most successful, followed by the MICP Inversion model and finally the Rho Simple model. The quality of fit at the MICP point of inflexion is better for the Rho Simple model. This is due to the use of the median pore diameter in Equation 3 to obtain the Rho Simple scaling factor. Median pore diameter is usually close to the point of inflexion in the MICP curves.

**Table 1:** Model fit quality for six selected samples

Plug	Nitrogen Permeability	NMR Porosity	Mean Delta Sw Rho Simple Model	Mean Delta Sw MICP Inversion Model	Mean Delta Sw Variable Rho Model
	mD	frac	Saturation Units	Saturation Units	Saturation Units
Plug A	1720	0.29	7.45	6.06	3.58
Plug B	552	0.33	9.90	4.55	1.93
Plug C	157	0.161	4.44	5.03	5.03
Plug D	7.15	0.28	5.33	5.29	3.75
Plug E	0.18	0.128	5.14	4.08	1.42
Plug F	0.05	0.08	2.73	2.96	3.15
<b>Sum of Delta Sw</b>			<b>34.99</b>	<b>27.97</b>	<b>18.86</b>
<b>Mean Delta Sw at Point of Inflexion</b>			<b>8.625</b>	<b>11.27</b>	<b>10.09</b>

It should be noted that the overall quality of fit values (Sum Delta Sw) listed in Table 1 depend on the distribution of  $T_2$  values or ‘bins’ in the  $T_2$  distribution. In the saturated sample  $T_2$  distributions the  $T_2$  times are distributed logarithmically, therefore there are more  $T_2$  bins at lower times. This means that the overall quality of fit values in Table 1 favour those models that have a better fit at low  $T_2$  times i.e. smaller pore/higher capillary pressures/high in the hydrocarbon column. Note that all modelled capillary pressure curves need to be converted to the appropriate fluid system for application in a given reservoir.

## CONCLUSION

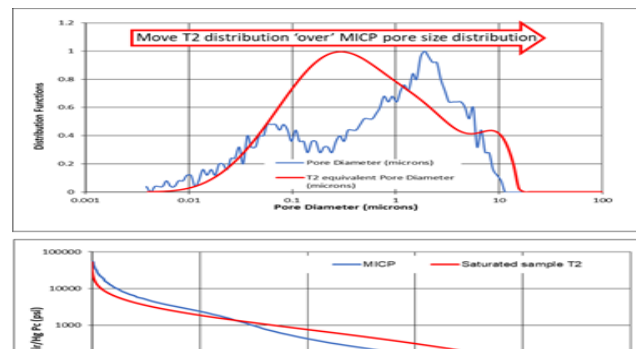
NMR and capillary pressure data from a large database has been used to construct and test different methods for modelling capillary pressure curves from saturated sample NMR  $T_2$  distributions. These models can be applied to NMR log data to convert the  $T_2$  distribution at each depth to a capillary pressure curve. The modelled capillary pressure curves can be used to estimate water saturation at each depth without the need to revert to a  $T_2$  cutoff or irreducible water saturation. Overall the variable scaling factor model is found to be the most successful. The use of single scaling factor models is found to be enhanced if the mercury injection data is inverted and handled in the same way than the NMR  $T_2$  data. This methodology will be more successful in gas or water-wet light oil reservoirs wells drilled with water-based muds with high degrees of mud filtrate invasion.

## ACKNOWLEDGEMENTS

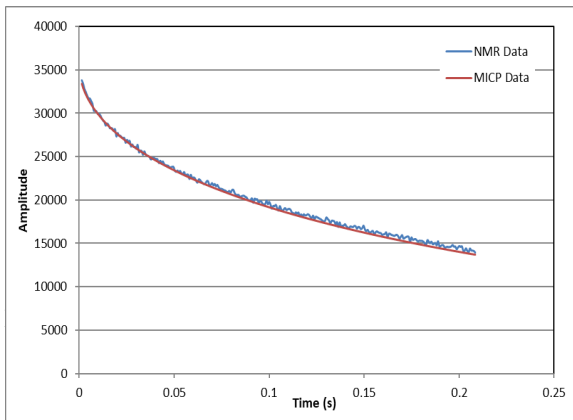
The authors would like to thank Weatherford Laboratories UK Ltd for access to and permission to use data from the ART NMR Sandstone Rock Catalogue.

## REFERENCES

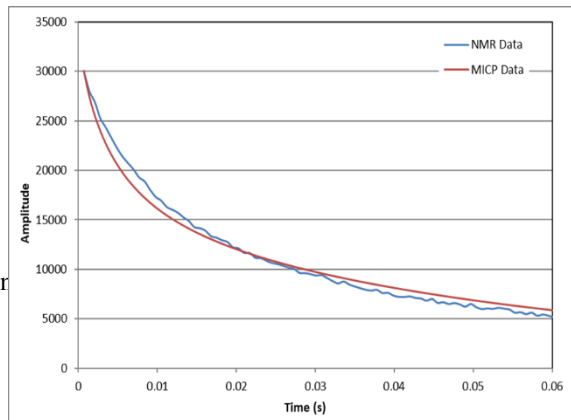
1. Walsgrove, T., Stromberg, S., Lowden, B. and Basan, P., 1997, "Integration of Nuclear Magnetic Resonance Core Analysis and Nuclear Magnetic Resonance Logs: An Example from the North Sea, UK. *SPWLA 38<sup>th</sup> Annual Logging Symposium*, 15-18 June 1997.
2. Marschall, D., Gardner, J.S., Mardon, D., Coates, G.R., "Method for Correlating NMR Relaxometry and Mercury Injection Data", Paper SCA1995-11, *Proc. Int. Symposium of Society of Core Analysts*, (1995).
3. Lowden, B.D., and Porter, M.J., "T2 Relaxation Time Versus Mercury Injection Capillary Pressure: Implication for NMR Logging and Reservoir Characterization" Paper SPE 50607, *SPE European Petroleum Conference, The Hague, (1998), Oct. 20-22*.
4. Volokitin, Y., Looyestijn, W.J., Slijkerman, W.F.J., Hofman, J.P., "A Practical Approach to Obtain Primary Drainage Capillary Pressure Curves from NMR Core and Log Data", Paper SCA1999-25, *Proc. Int. Symposium of Society of Core Analysts*, (1999).
5. Coates, G., Xiao, L., and Prammer, M., *NMR Logging Principles & Applications*, Halliburton Energy Services, 1999.
6. Shafer, J. and Neasham, J., "Mercury Porosimetry Protocol for Rapid Determination of Petrophysical and Reservoir Quality Properties", Paper SCA2000-21, *Proc. Int. Symposium of Society of Core Analysts*, (2000).
7. Lenormand, R., "Interpretation of Mercury Injection Curves to Derive Pore Size Distributions", Paper SCA2003-052, *Proc. Int. Symposium of Society of Core Analysts*, (2003).
8. Brandimarte, F., Eriksson, M. and Moss, A., "How to Obtain Primary Drainage Capillary Pressure Curves Using NMR T2 Distributions in a Heterogeneous Carbonate Reservoir," Paper SCA2017-066, *Proc. Int. Symposium of Society of Core Analysts*, (2017).
9. Amaefule, J. O., Altunbay, M., Tiab, D., Kersey, D.G. and Keelan, D.K., "Enhanced reservoir description: using core & log data to identify hydraulic (flow) units & predict permeability in uncored intervals/wells", 1993, SPE No. 26436.



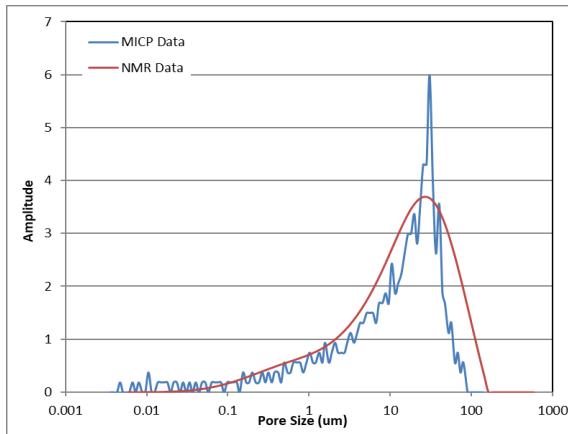




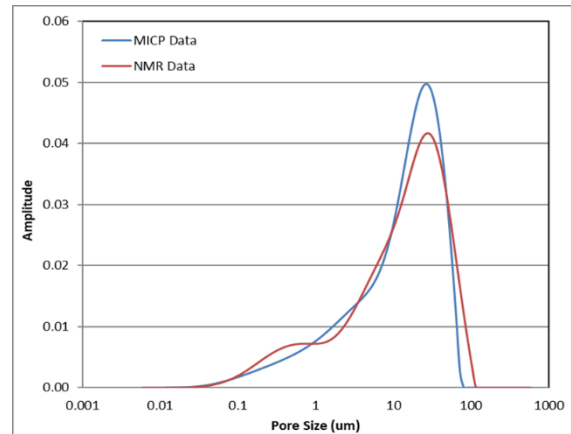
**Figure 2a:** Example of a good match between MICP & NMR in the time domain.



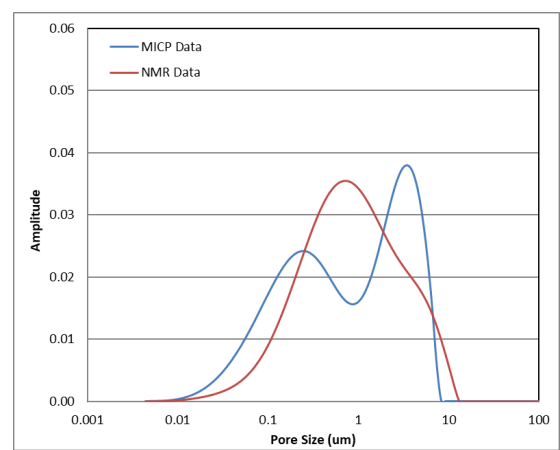
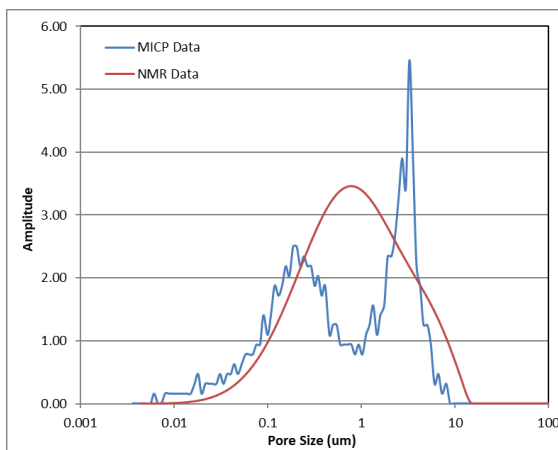
**Figure 2b:** Example of a poor match between MICP & NMR in the time domain.



**Figure 3a:** Comparison of the 'raw' MICP pore size and T2 distributions for the sample used in Figure 2a.



**Figure 3b:** Comparison of the pore size and T2 distributions for the sample used in Figure 2a after time domain matching in inversion.



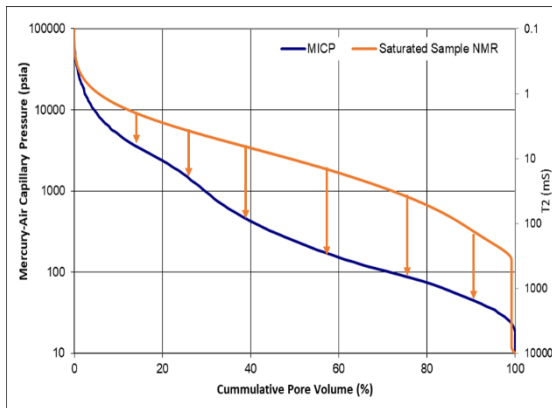


**Figure 5:** This plot demonstrates that it is possible to convert each  $T_2$  time to a given capillary pressure.

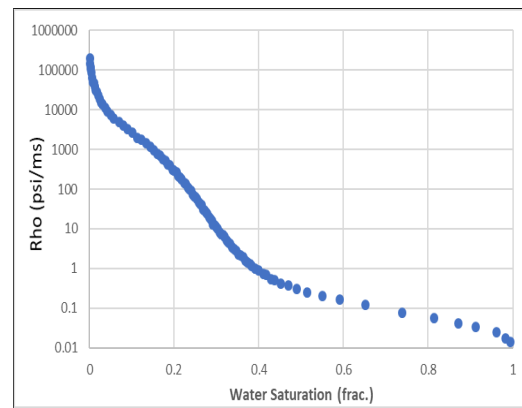


**Figure 6:** An example of scaling factor (Rho) versus saturation.

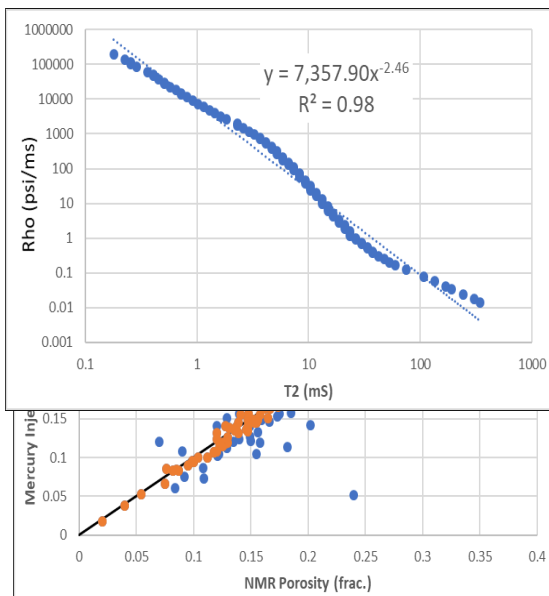


**Figure 4a:** Comparison of the 'raw' MICP pore size and  $T_2$  distributions for the sample used in Figure 2b.

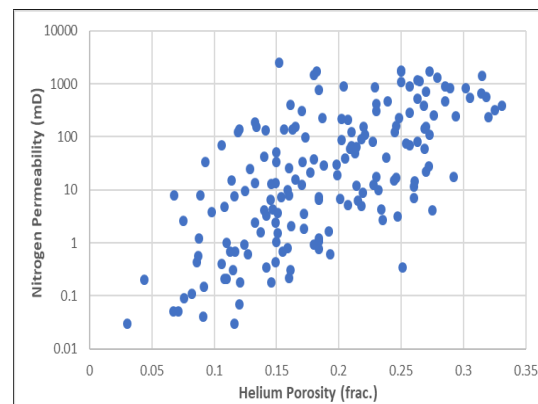


**Figure 8:** Nitrogen permeability versus helium porosity for the 174 plugs used in this study.

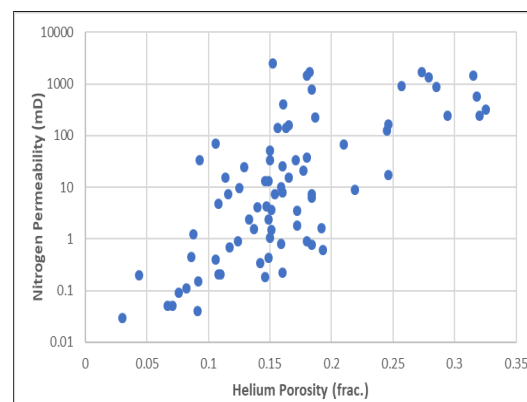


**Figure 4b:** Comparison of the pore size and  $T_2$  distributions for the sample used in Figure 2b after time domain matching in inversion.

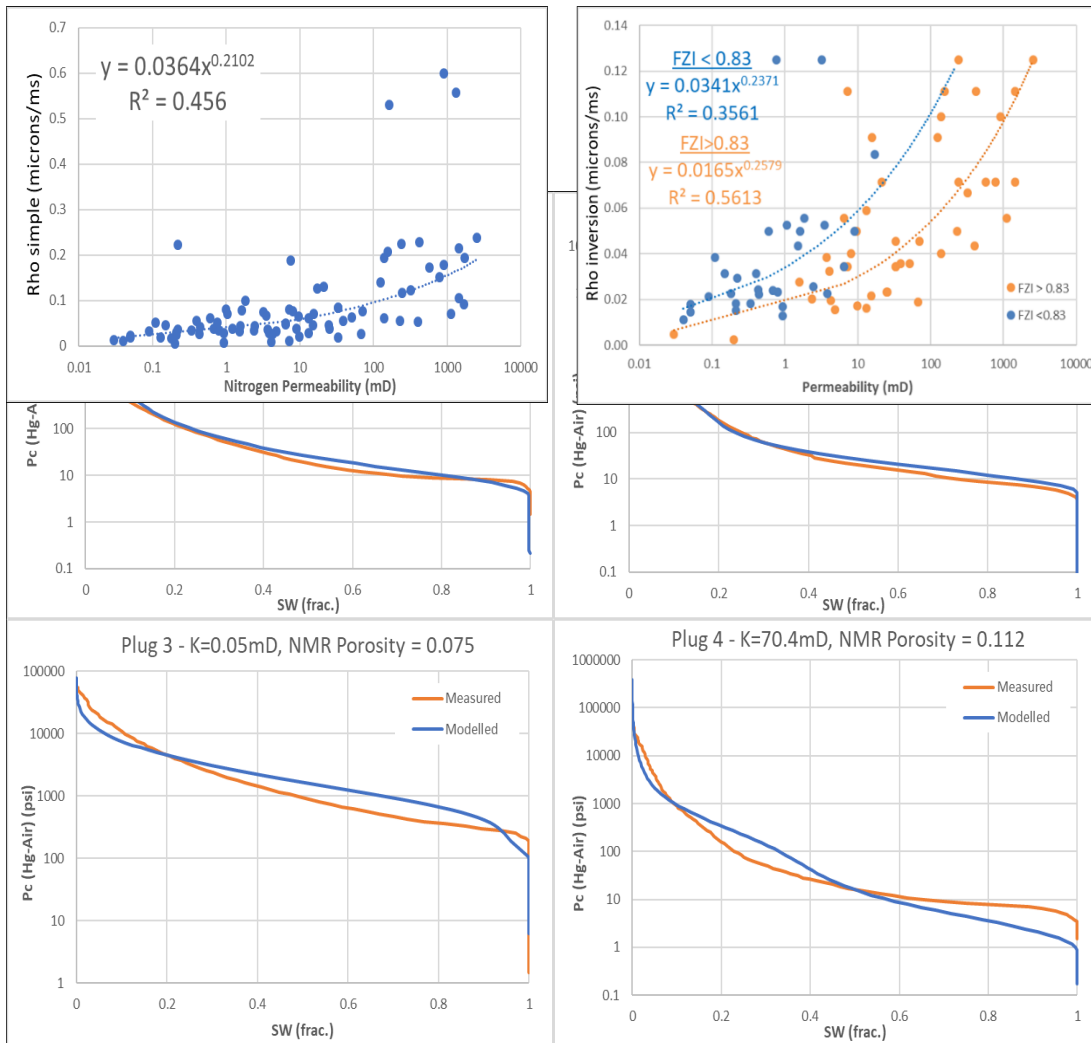


**Figure 9:** Mercury injection porosity versus NMR porosity.

**Figure 10:** Nitrogen permeability versus helium porosity for the 78 plugs with a difference between NMR and MICP porosity less than 0.015.

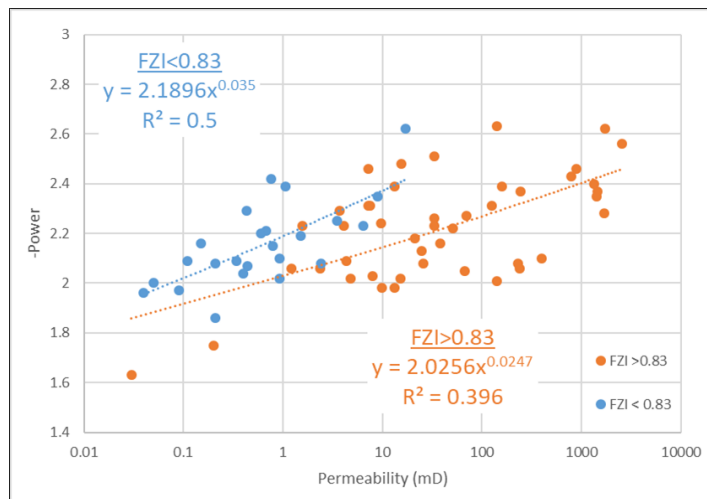


**Figure 14:** Variable Rho 'power' values versus permeability for two FZI groups.

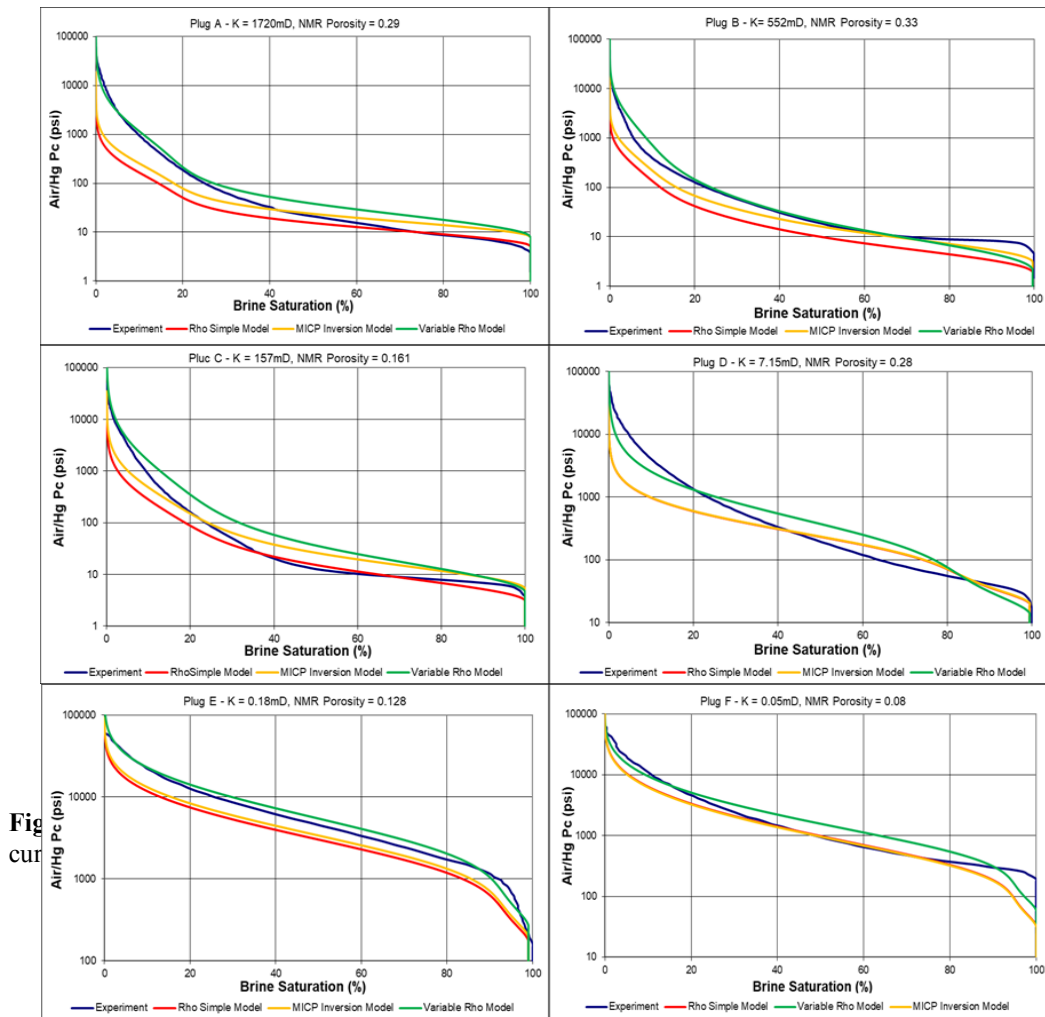


**Figure 15:** Modelled versus measured mercury injection curves using the three scaling factor models for six plugs sample.